Reaction Barriers: Origin and Evolution

Neil M. Donahue*

Departments of Chemistry and Chemical Engineering, Carnegie Mellon University, Pittsburgh, Pennsylvania 15213

Received February 3, 2003

Contents

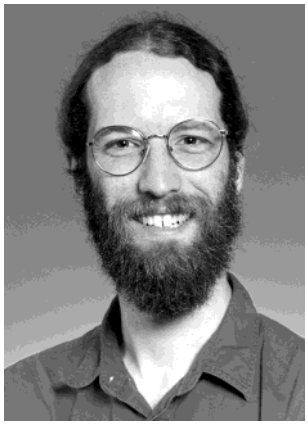

Neil Donahue is an Assistant Professor of Chemistry and Chemical Engineering at Carnegie Mellon University. He was born in Pittsburgh, Pennsylvania, in 1963. He received an A.B. in physics from Brown University in 1985 and a Ph.D. in meteorology (atmospheric chemistry) from the Massachusetts Institute of Technology in 1991, working with Professor Ronald Prinn. From 1991 to 2000, he directed kinetics research in Professor James G. Anderson's group at Harvard University. He has been at Carnegie Mellon University since 2000. His research interests span a wide area, ranging from theoretical treatments of chemical reactivity, through experimental kinetics, to atmospheric measurement of radicals and reduced material in multiple phases.

1. Introduction

1.1. Background

Most bimolecular reactions involving at least one closed-shell species exhibit a *barrier*. Here we shall focus on radical−molecule reactions. Barriers are ubiquitous because all radical−molecule reactions involve a dramatic transformation in the ground-state wave function Ψ^G during the transition from reactants Ψ_R^G to products Ψ_P^G (Figure 1). In most cases the products of a radical−molecule reaction are again a radical and a molecule, but with very different nuclear geometries—after all, a chemical reaction has occurred.

A great deal of the early understanding of chemical reactivity following the development of quantum mechanics focused on key aspects of this transformation from reactant to product states. This began with London's treatment of H + H_2[1] and essentially culminated in the work of Fukui[2] and Woodward and Hoffman,[3] which formalized the quantitative analysis of frontier-orbital interactions and orbital-overlap calculations informed by symmetry arguments. However, there is not a clean connection between the concepts and definitions of the quantum states in these treatments and the corresponding states resulting from the Hartree−Fock self-consistent field (SCF) states underlying modern ab initio computations. This is because the SCF molecular orbitals span the complete system, including all reactant and product species, and the resulting excited states do not easily map onto the excited states of the individual, separated reactants and products, which are the basis for the earlier work. There are several solutions to this problem: one is to use valence-bond theory, with its focus on breaking and forming bonds;[4,5] another is to develop a form of asymptotic matching to relate states of the isolated reactants and products to states near the saddle point.[6]

The emphasis in this review will be to draw on this latter work to build a picture of the variation of chemical reactivity observed in atmospheric chemistry. We will focus on variation in two forms: simple differences in rates—why one reaction is faster than another; and transformations in behavior—why seemingly similar reactions exhibit grossly different behaviors, for instance changing from "normal" Arrhenius reactions to reactions with a strong negative temperature dependence.

1.2. Barriers

The functional definition of *barrier* varies. Several important (and related) quantities are sometimes referred to: the local maximum in the electronic potential energy surface along the reaction coordinate (we shall call this the *Born−Oppenheimer barrier*);

* Phone: (412) 268-4415. Fax: (412) 268-7139. E-mail: nmd@andrew.cmu.edu.

10.1021/cr020650g CCC: $44.00
Published on Web 11/14/2003

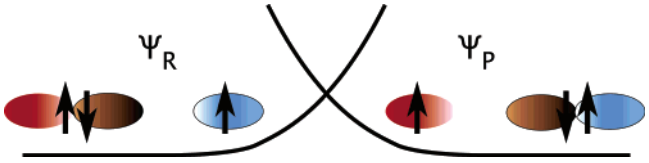

Figure 1. Basic schematic of a radical−molecule reaction, focusing on three electrons in the HOMO of the molecule and the LUMO of the radical. The reaction clearly involves a transformation from a reactant ground state Ψ_R to a product ground state Ψ_P.

the local maximum in the ground-state energy, including vibrational zero-point effects (this is generally called the *vibrationally adiabatic barrier*); the *free energy barrier*, which includes entropic effects in the adiabatic barrier; and the local slope in a standard ln k vs $1/T$ Arrhenius plot (the *activation energy*). The factors contributing to and governing barriers are the primary subject of this review, but equally important are the relationships among these various definitions. From a practical standpoint we are most interested in the last term—the activation energy—as that is what is observed with thermal kinetics and what determines how rate constants change in thermal environments, such as the atmosphere. However, in spite of the Boltzmann-like term, $\exp(-E_a/RT)$, the activation energy is rather loosely related to the more fundamental barriers. Computations such as ab initio calculations and theories such as curve-crossing treatments both describe the first term—the Born−Oppenheimer barrier—most directly. It is not straightforward to move in either direction—to deduce the Born−Oppenheimer barrier from measured rate constants, or to calculate a thermal rate constant from computed electronic potential energy surfaces.

It is important to realize that the local potential energy maximum need not be at a higher energy than the separated reactants; it may be "submerged" due to stabilizing effects near the transition state, resulting in strongly non-Arrhenius behavior and negative activation energies. However, the physics depicted in Figure 1 guarantees that essentially all radical−molecule reactions will have a barrier of some sort; only a combination of very low crossing heights and very strong coupling, discussed below and depicted in Figure 2, can effectively erase a barrier from a reaction coordinate. This circumstance will be discussed in detail below.

This volume is devoted to atmospheric chemistry, and so we shall focus on questions related to that field. There are several reasons to strive for a complete understanding of the subject (barriers). First is the wide dynamic range of temperature and pressure in the atmosphere. Considering only the troposphere and stratosphere, temperature ranges from approximately 330 K to approximately 180 K, while pressure ranges from 1030 mbar to 1 mbar. Furthermore, chemistry under some of the extreme conditions can be very important—for instance, the coldest temperatures are found near the tropopause, and the chemistry of the upper troposphere/lower stratosphere is of great importance. Because of the wide range of conditions, we often need to extrapolate experimental data, and this requires a good theoretical foundation. Second is the inference we may draw on reaction *mechanisms* from kinetic data. Many atmospheric species, in particular organic compounds, have multiple possible reaction pathways, and we occasionally need to draw mechanistic conclusions from the kinetic data. This again requires a good theoretical foundation. Third is the status of "pathological" reactions. Some rate constants do not obey obvious empirical trends, and we must decide whether to believe the data and, when we are satisfied, to what extent seemingly similar reactions will display similar pathology. Once more, this requires a good theoretical foundation.

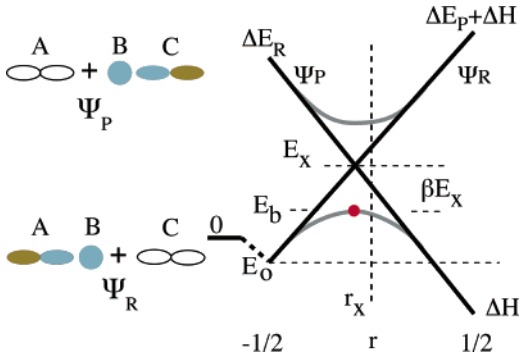

Figure 2. Reaction as an avoided curve-crossing, mixing states Ψ_R, the reactant ground state, and Ψ_P, the product ground state, using a simple atom transfer (AB + C → A + BC) as an example. The coordinate r is similar to a mixing angle. It is generally driven by deformations associated with the chemical transformation (transfer of B in this case). Along this deformation coordinate, the diabatic energies of Ψ_R and Ψ_P are assumed to evolve linearly, resulting in a curve-crossing at some energy E_x. The important boundary conditions are the ground-state energy of the reactants, E_0, the reaction enthalpy ΔH, and the initial and final gaps between ground and excited-state energies, ΔE_R and ΔE_P. The *barrier* (E_b) is formed by the coupling of these states, which splits the energies at the crossing, as shown. The coupling is expressed as a fraction of the crossing energy, βE_x, where β is typically 0.8−0.9 for the strongly coupled systems considered here.

2. Theoretical Considerations

In this section we shall review the various aspects connecting the electronic potential energy surface to thermal rate constants, focusing at each turn on how various reactions differ from each other—in other words, on the derivative.

2.1. Curve Crossings

It has been recognized since Heitler and London's treatment of $H + H_2$[1] that chemical reactions can be treated as avoided curve-crossings. This is the fundamental underpinning of most major theoretical treatments of reactivity.[4−9] Put simply, the ground-state wave function of the reactants Ψ_R^G is not the same as the ground-state wave function of the products Ψ_P^G, but states cannot vanish; consequently, each ground state must correlate to a corresponding excited state on the opposite side of the reaction coordinate. This is depicted in Figure 2 for a simple atom-transfer reaction, AB + C → A + BC. Schematics for the reactant and product wave functions are shown to the left of the crossing diagram. The essence

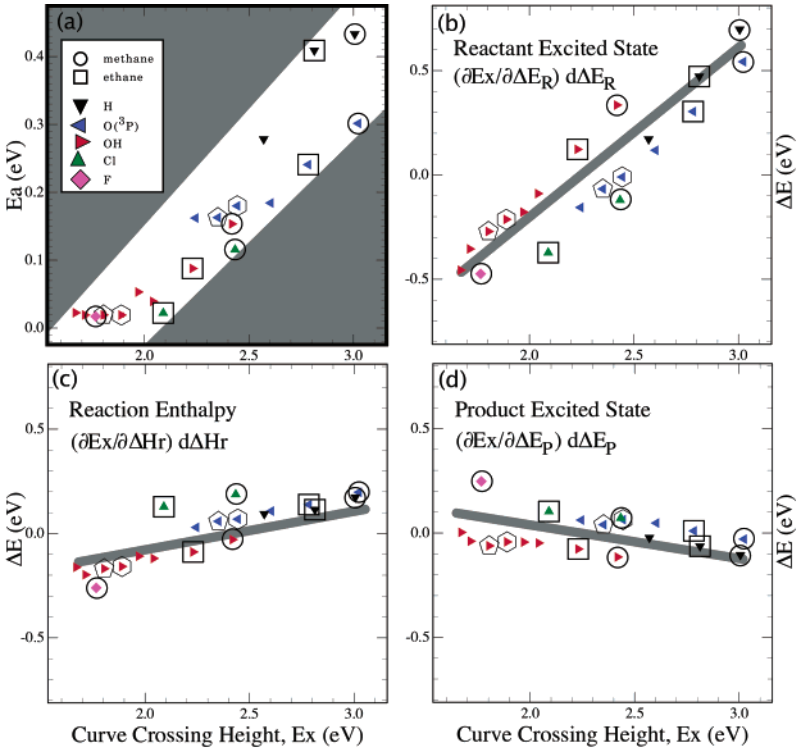

Figure 3. (a) Experimental activation energy vs crossing height for hydrogen-atom-transfer reactions from alkanes. Radicals are indicated by the filled symbol shape and color, while alkanes are indicated by the surrounding open symbol, as shown in the legend. Only some molecules are identified (the pentagon and hexagon are cyclopentane and cyclohexane, for example). The common evolution of radical and molecule reactivity is a key success. (b−d) The contributions of variations in each of the three major boundary terms to the overall variation in crossing height: (b) the reactant excited-state energy gap, (c) the reaction enthalpy, and (d) the product excited-state energy gap. In these systems, the reactant energy gap dominates the variation in barrier heights, as shown by the much greater values in (b) than (c) or (d).

of the problem is this: starting at some boundary condition, as the reaction proceeds the energy of the ground state increases, while the energy of some excited state decreases. Eventually, the two energies converge and the two states cross at some energy E_x. Overlap between the two wave functions will generate splitting along this reaction coordinate, resulting in a hyperbolically shaped adiabatic surface.[9] The resulting maximum energy E_b is the Born−Oppenheimer barrier height, and it can be written as a function of the crossing height and a nondimensional splitting parameter β:

$$E_b = E_x - \beta E_x = (1 - \beta)E_x = \gamma E_x \qquad (1)$$

Most reactions of interest in atmospheric chemistry are strongly coupled; they have a large splitting term ($\beta = 0.8-0.9$, $\gamma = 0.1-0.2$) coupling the reactant and product states[9] and a correspondingly low barrier, allowing reasonably fast reactions at ambient temperatures.

The first-order problem in understanding barrier heights is to understand this crossing height. In turn, the primary realization is that the problem is dominated by the excited-state energies. For a linear crossing, the crossing height is[6]

$$E_x = \frac{\Delta E_R(\Delta E_P + \Delta H)}{\Delta E_R + \Delta E_P} \qquad (2)$$

with respect to the initial ground-state energy E_0. This simple expression describes the evolution in barrier heights in a very wide range of radical−molecule reactions, as we shall demonstrate here. For example, Figure 3 shows the tight relationship between observed activation energies and the crossing heights predicted by eq 2 for H-atom-transfer reactions from alkanes to a series of radicals. It also shows the dominance of a single term in eq 2—the excited-state energy gap of the reactants, ΔE_R. There is no clear reason why this one term should dominate. It happens that excited-state energies are typically larger and more variable than reaction enthalpies, and quite frequently the reactant excited-state energy gap is significantly smaller than the product gap. The common intuition that barriers should relate to reaction enthalpy is misguided—it turns out to be true in some cases but dramatically false in others. In turn, our intuition about chemical behavior, expressed in statements like the Hammond postulate,[10] is violated when the typical behavior shown in Figure 3 breaks down.[11]

We often discuss these energies in terms of a zero-energy boundary condition for the reactant ground state—in other words, the crossing problem is assumed to begin at the energy of the separated reactants. This is in fact frequently not a good assumption. The difference between the energy of the reactants and the initial energy of the crossing problem, E_0, can profoundly influence not just the rate but the whole behavior of a reaction,[12] as we shall see later. This is particularly true when there is enough stabilization (E_0 is low enough) that the barrier is actually below the reactant energy.

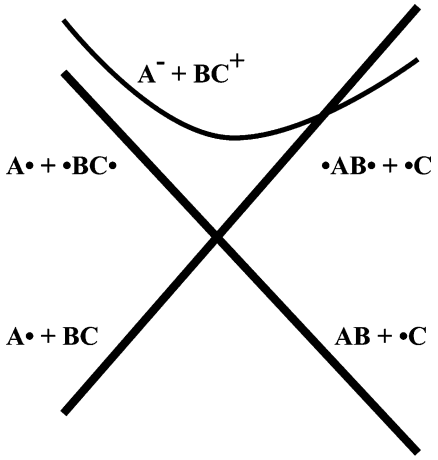

Figure 4. Ionic excited states in the valence-bond avoided curve-crossing model of Shaik and Pross. The diabatic two-state problem is described in terms of singlet−triplet splittings for the molecular species (i.e., AB vs ·AB·). Mixing with a charge-transfer state ($A^- + BC^+$) is a second-order term.

2.1.1. Boundary Conditions

We have so far ignored what controls the boundary conditions in the curve-crossing model. There are several approaches. Marcus theory[8] is appropriate for weakly coupled systems ($\beta \ll 1$) where the reaction coordinate is dominated by motions other than reactant nuclear distortion. The seminal case is electron transfer, where the reaction coordinate is solvation-shell fluctuations. In this case the diabatic ground states are not linear but rather quadratic, and the entire problem reduces to two overlapping parabolas. Variations in barrier height in a homologous series reduce to changes in reaction enthalpy.

This picture of reactivity precedes Marcus[13] for atom-transfer reactions, originating in the work of Evans and Polanyi[7] for metal−alkyl halide reactions. It is not appropriate, however, for strongly coupled reactions because the excited-state energy is effectively ignored (it is replaced by the null-reaction coupling constant λ).

In physical organic chemistry, a mature theory has emerged from the work of Pross and Shaik.[4,5] The basic curve-crossing in eq 2 is established, for radical−molecule reactions, by an excited state incorporating the triplet excited state of the molecule, in a valence-bond formalism. This corresponds to promoting a bonding electron in the breaking bond into an antibonding state that mixes with the singly occupied orbital of the radical to form a new bond (see Figure 4). It is thus intuitive and well grounded. In many systems, the basic energetics of the singlet−triplet splitting are nearly constant across a homologous series, so the effect of the interaction is to establish an adiabatic barrier, E_b, which is then subject to perturbations from other interactions to form an ultimate barrier E_b'. These perturbations correspond neatly to the interactions described empirically by Hammett parameters.[14] Of particular interest is the polar effect, associated with Hammett's σ^+, which is frequently interpreted as relating to charge separation at the transition state induced by mixing with an excited ionic surface.[15,16]

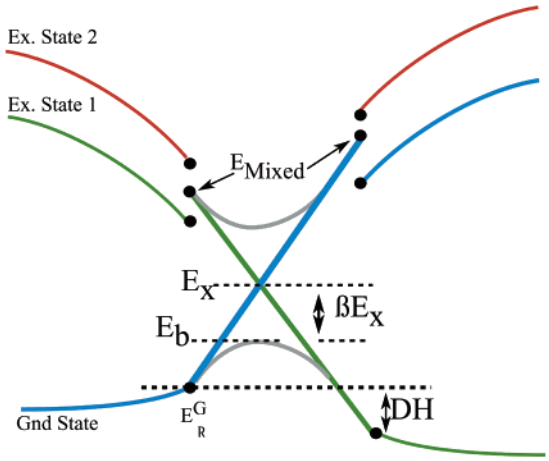

Figure 5. Two-state avoided curve-crossing bounded by mixed excited states. The mixed-state energy is based on the contribution of each excited state to the delocalization energy—i.e., the coupling of each state with the ground state. The subsequent two-state avoided curve-crossing is identical to Figure 2.

An alternative is to mix the excited states at the boundary of the curve-crossing,[17,18] shown in Figure 5. This is valid only in the strong-coupling limit, where the individual diabatic states of the reactants and products are completely transformed at the saddle point. This is, however, the limit of interest here. The mixing terms are calculated from the (small) frontier-orbital delocalization energy at the onset of significant frontier-orbital overlap S_i (for state i).

$$D_i = \frac{S_i^2}{E_i} \tag{3}$$

For instance, with two excited states in question, a mixed excited-state energy is a weighted average of the excited-state energies,[19]

$$E_{mix} = \frac{\sum_i S_i^2}{D} \tag{4}$$

where D is the total delocalization energy between the ground state and all relevant excited states. It is necessary for a variational treatment of barrier heights to *lower* the barrier with each added interaction. In this strongly coupled case this is satisfied if the splitting term, γ, is large and proportional to the frontier-orbital overlap, S^2.

In fact, as we shall see, three basic factors—variation in excited-state energies, variation in the coupling, and variation in the ground-state energy E_0—are responsible for the great bulk of observed behavior in radical−molecule systems. Excited-state energy differences drive the basic variation in reactivity in a homologous series, such as the H-atom transfers illustrated in Figure 3. Ethane is more reactive than methane because of a lower ionization potential, while chlorine atoms are more reactive than OH because of a higher electron affinity—in each case the effect is to lower the reactant excited-state energy gap ΔE_R. Variation in coupling is

responsible for the apparently exceptional behavior of some compounds. A good example is the reactivity perhaloalkenes. The reduced reactivity (and thus increased environmental persistance) of the haloalkenes is driven by reduced frontier-orbital overlap between the highest occupied molecular orbital (HOMO) of the molecule and the lowest unoccupied molecular orbital (LUMO) of the attacking radical.[19−21] The effect is a reduced splitting at the avoided crossing. Finally, the effect of changing the initial energy, E_0, can be dramatic. Most notably, when this initial energy drops well below the energy of the separated reactants, generally due to a combination of van der Waals and hydrogen-bonded complexes, reactions can exhibit a dramatically inverse temperature dependence, with greatly increased rates at low temperature.[12]

2.2. Rate Constants vs Barriers

Before we proceed to study specific systems, we need to consider the connection between barrier heights and the overall rate constant. These turn out to be very closely related. The Arrhenius activation energy differs from the adiabatic barrier for two reasons: the Arrhenius *A*-factor depends on temperature, sometimes strongly; and tunneling varies with energy and thus temperature. In this review we will assume that the broad behavior of the reactions under discussion can be understood in terms of statistical theories. In fact, one can understand the overall rate constant with a highly reduced form of transition state theory.[11] This formulation focuses on key modes undergoing a substantial transformation as the system moves from reactants to the transition state—for example, reactant translation orthogonal to the reaction coordinate becomes rotation at the transition state, and the rotations of the individual reactants become bending vibrational modes. Almost all of the other vibrational modes of the reactants are spectators—their only significant role, if they have one, is to change the overall zero-point energy of the system. We can thus write a relatively simple expression for the rate constant (in cm^3 $molecule^{-1}$ s^{-1}, with frequencies in cm^{-1}):

$$k = \frac{B\kappa(T,\nu_i)g(T)\left[10^{-9}S\mu^{-3/2}\sqrt{I_{TS}^3/(I_{rad}I_{mol}^3)}\right]e^{(-(E_b+\Delta E_{zp})/T)}}{(1-e^{-1.44\nu_1/T})^2(1-e^{-1.44\nu_2/T})(1-e^{-1.44\nu_3/T})T} \quad (5)$$

This equation applies to linear radicals (i.e., OH).

The key parameters of eq 5 follow: *B* is a prefactor including the effect of all neglected terms—because those are spectators, *B* is near unity. κ is a tunneling coefficient. *g* is the ratio of electronic degeneracies of the transition state and the radical. *S* is the overall symmetry factor for the reaction—the number of identical reaction pathways. μ is the collisional reduced mass, in amu. I_{TS}^3 and I_{mol}^3 are the products of the moments of inertia of the transition state and the reactant molecule ($I_AI_BI_C$), in amu-Å^2. I_{rad} is the moment of inertia of the radical. In this form we assume that one rotational degree of freedom for the radical is preserved at the transition state, which is manifestly not true in some important cases; the rotation is nearly always hindered, and in the hydrogen-bonded examples discussed below it is completely frozen. ν_1 is a bending mode related to the impact parameter of the radical−molecule collision; it is often the lowest frequency mode. ν_2 is the symmetric stretch of the radical approaching the molecule. ν_3 is the bending mode resulting from the lost rotational mode of the radical. ΔE_{zp} is the overall change in zero-point energy between the reactants and the transition state—it is driven in part by the three vibrations just described, but also by the lost molecular vibration that is the atom-transfer reaction coordinate (a C−H stretch for alkanes, where $\Delta E_{zp} \simeq -3000$/cm or -2000 K), as well as any other frequency changes at the transition state.

The inertial terms, contained in square brackets in the numerator of eq 5, can be determined to very high accuracy using low-level ab initio or semiempirical calculations. The tunneling coefficient, κ, is based on Truhlar's one-dimensional function:[22]

$$\kappa(T) = \begin{cases} \dfrac{T_t/T}{T_t/T-1}\left(\exp\left[\left(\dfrac{T_t}{T}-1\right)\dfrac{T_b}{T_t}\right]-1\right) & T \le T_t \\ \dfrac{\pi T_t/T}{\sin(\pi T_t/T)} - \dfrac{T_t/T}{1-T_t/T}\exp\left[\left(\dfrac{T_t}{T}-1\right)\dfrac{T_b}{T_t}\right] & T > T_t \end{cases} \quad (6)$$

where $T_b = E_b + \Delta E_{zp}$ is the barrier height in *K* and T_t is a tunneling temperature related to the imaginary frequency: $T_t = \hbar\omega_i/(2\pi k_B)$. The tunneling temperature is the temperature *below* which $\kappa \gg 1$.

A crucial theoretical finding is that the three most important parameters in eq 5, E_b, T_t, and ν_1, are highly correlated.[11] In particular, the considerations described above that drive variations in the barrier height simultaneously drive variations in the imaginary frequency (and thus T_t) and in the TS bending frequency (ν_1). As the barrier lowers from one reaction to the next, the reaction channel gets wider and the barrier gets relatively broader. This is because these terms all arise from the frontier-orbital interactions discussed above; the bending, for example, is defined by a quadratic energy rise from the transition-state minimum as frontier-orbital overlap decreases away from the optimal orientation. The absolute curvature is thus a dimensionless overlap term scaled by the crossing energy; as the crossing height drops, so does the bending frequency. This is responsible for the emergence of "stripping" behavior seen in low-barrier reactions, such as Cl + ethane.[23] It is also why there is usually a tight relationship between barriers and *A*-factors. The theoretically derived correlations among the parameters permit well-constrained fitting of rate data to functions of this form. This in turn provides a much tighter link between rate data and theoretically derived barriers.[11,24] In particular, the E_b parameter obtained from a fit using eq 5 *is* closely related to a Born−Oppenheimer barrier, whereas the E_a obtained from a log-linear Arrhenius fit is not.

3. Discussion

In this section we shall discuss several systems of interest to atmospheric chemistry, each of which also illustrates a facet of the overall reactivity theory just presented.

3.1. Atom Transfers

Many oxidation processes are initiated by atom-transfer reactions. Hydrogen-atom transfers are most prominent. They form the basis of this treatment, and so have already been discussed here. Figure 3 shows the evolution in H-atom abstraction barriers from alkanes by a series of radicals (H, O(^{3}P), OH, Cl, F). The plot is of measured barrier (based on a fit similar to eq 5) vs predicted crossing height, using only the ionic state defined by $IP_{molec}-EA_{rad}$. For this main sequence, barrier-height variation is driven almost entirely by variation in the reactant ionic state, as shown in the subsequent panels of Figure 3. The coupling constant $\gamma = 1 - \beta$ is approximately 0.75 (the slope of the data in Figure 3a is ≃0.25), which is consistent with theoretical predictions.[9]

It is important to note that, for this discussion, the "barrier" is always reported in the exothermic direction for reactions that display a significant heat of reaction. Equation 2 is appropriately symmetric, but it is uninformative to talk about a substantially endothermic reaction as having a high barrier. A case in point is the reaction $Br + C_2H_6 \rightarrow HBr + C_2H_5$. One might naively expect it to have a low barrier as written because of the high electron affinity of Br and the (relatively) low ionization potential of ethane. Of course, however, the reaction is endothermic. The reverse reaction, however, does indeed show a very low (possibly negative) barrier,[25−27] though the exact rate constant for the reaction is controversial.

The R + HBr reactions are a very interesting example, because the low barrier is driven by a low energy gap in the *product* channel, as opposed to the more usual examples presented in Figure 3, where the barrier is governed by the *reactant* energy gap. Much chemical intuition, it turns out, is based on the more common case of reactant-side control, and so we can expect these product-side-controlled reactions to appear pathological. This is the case. In particular, there is increased room for pre-reactive interactions in the entrance channel. Combined with the large dipole moment of HBr, this enables the formation of a significantly stabilized van der Waals complex, which in turn permits the barrier to form below the reactant energy. This is the first example of a system where the initial energy, E_0, can play a critical role. It is also an example of a reaction that violates the Hammond postulate[10]—the transition state is late and yet is near in energy to the reactants. Barrier location in fact has nothing to do with the reaction energy—it is driven by the asymmetry of the reactant and product excited-state energy gaps.[11]

Another H-atom transfer plays a crucial role in atmospheric oxidation chemistry. This is the occasional abstraction of H atoms by molecular oxygen. In particular, the abstraction of an H from alkoxy radicals by molecular oxygen to form HO_2 and a carbonyl ($RO + O_2 \rightarrow R'{=}O + HO_2$) plays a key role in hydrocarbon oxidation. There are three prominent fates for alkoxy radicals, and so variation in barrier height along one of the pathways helps control the branching. Molecular oxygen has a high electron affinity (2 eV) and thus should be a "good" radical, yet it seldom reacts with reduced material at ambient temperatures. This is because most candidate reactions (leading to HO_2) are endothermic. When reaction enthalpy allows, the reaction proceeds. The general pattern of activation energies in this series progresses from $E_a/R = +1080$ K for O_2 + methoxy, +550 K for ethoxy,[28] to recently observed negative activation energies (∼ −500 K) for butoxy and pentoxy radicals.[29,30] A full analysis would require, among other things, detailed knowledge of the ionization potentials of these radicals, but the general trend is consistent with the behavior we have seen in other reactions.

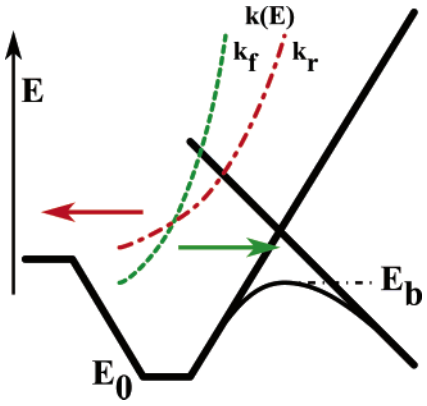

Figure 6. Ingredients for a negative temperature dependence. A pre-reactive interaction (such as H-bonding) stabilizes a pre-reactive complex (E_0), driving the barrier (E_b) below the reactant energy. Microcanonical forward (k_f, green dotted line) and reverse (k_r, red dashed line) rate constants out of the complex evolve differently with energy, with k_r rising much more rapidly than k_f. When k_f has a significantly lower threshold energy, the forward rate will dominate at low energy, and so formation of products will be favored at low temperatures.

3.1.1. Negative Temperature Dependencies

The importance of reactions with a strong negative temperature dependence became clear with the experimental work on OH + $HONO_2$ in the early 1980s.[31] This crucial reaction, which is the major true sink of odd-hydrogen radicals in the stratosphere, is dramatically faster at low temperature; the rate constant is more than an order of magnitude larger at 200 K than at 300 K.[32] Consideration of this reaction led to the basic two-transition-state mechanism shown in Figure 6,[33,34] but the nature of the pre-reactive complex remained controversial for many years, and the dual-transition-state mechanism was regarded as something anomalous.

Other evidence has emerged recently suggesting that pre-reactive complexes are commonplace, especially with the OH radical, which can form hydrogen bonds and also has a large dipole moment. Experimental work in reaction dynamics has shown that van der Waals complexes can be stabilized in the entrance channel of the OH + methane system.[35] The

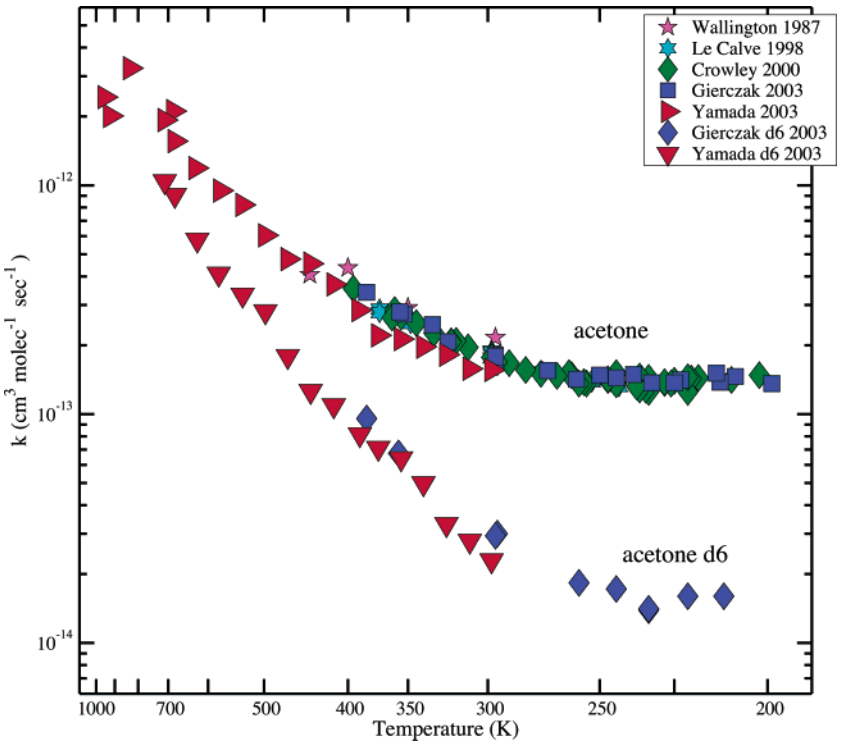

Figure 7. Temperature-dependent data for OH + acetone and OH + acetone-d_6 showing strong non-Arrhenius behavior. Rate data show clear curvature at low temperature and a very strong primary kinetic isotope effect. The kinetic isotope effect at all temperatures confirms that H-atom abstraction dominates. The reaction thus appears to proceed via two quantum-mechanically distinct pathways involving abstraction from the methyl group. A non-H-bonded transition state reflects "normal" abstraction from a methyl group, with a high *A*-factor and a high activation energy. This dominates at high temperature. Hydrogen bonding with ketonic oxygen stabilizes but tightens a second transition state, lowering the *A*-factor by 2 orders of magnitude but also generating a negative activation energy. This dominates at low temperature because of the sharply lowered barrier.

van der Waals complexes presumably exist in essentially all H-atom abstraction reactions involving reactants with large dipole moments and polarizabilities. Their role may be subtle—essentially a modest stabilization reducing the barrier height of the reaction—or it may be pronounced—contributing to a negative activation energy in reactions like ethyl + HBr discussed above.

Hydrogen bonding has also been discussed as a source of pre-reactive complexes in OH reactions. In addition to the OH + $HONO_2$ reaction, many rate constants involving OH and oxygenated hydrocarbons show a degree of "anomalous" behavior. For example, a succession of studies on the kinetics of oxygen-containing organics have revealed progressively more negative temperature dependences in a series of substituted aldehydes.[36]

Smith and Ravishankara[12] have presented a persuasive case that hydrogen-bonded complexes can play a significant role in reactions involving OH, including a much more detailed discussion of the evidence presented above. In the context of the discussion here, there are two major effects of these complexes. First, the considerable binding energy of the complexes drives E_0 well below the reactant energy—often by enough to lower the barrier itself below the reactant energy. This causes a negative temperature dependence in the kinetics. Second, the hydrogen-bonded ring structure of the transition state disrupts the nearly free OH rotation included in eq 5, replacing it with a relatively stiff vibration. This lowers the pre-exponential factor substantially.

Reactions such as the "normal" H-atom transfers we have considered are reasonably easy to understand in the context of transition state theory. A pre-reactive complex changes this dramatically. Now we must consider both formation and decay of the complex as well as collisional energy transfer. A schematic for the reaction is shown in Figure 6. In addition to the curve-crossing and pre-reactive complex, we show the *microcanonical* rate constants, $k(E)$, for unimolecular decay of the complex back to reactants (k_r, red) and forward to final products (k_f, green). Because the reverse reaction is barrierless, the sum of states at the transition state (and thus the microcanonical rate constant) rises very rapidly with energy. The tighter transition state for forward reaction (and it is very tight because of the hydrogen bonds) shows a much more gradual rise in $k(E)$ with energy. However, because the forward reaction has a lower critical energy, it is favored at low energy—thus the low energy (low temperature) preference for the forward pathway. Finally, the overall loss rate for the pre-reactive complex ($k_r + k_f$) is often similar to or faster than the collision rate, so energy transfer must be considered, and the rate will display a pressure dependence. The appropriate vehicle is the master equation.[37−39]

It is very important to realize that this transformation from a "simple" reaction to a "complex" reaction is completely smooth. There is no fundamental shift in mechanism, only an evolution in the balance of terms that control the transition-state energetics. Pre-reactive complexes exist in many systems, but

the "pathalogical" behavior emerges only when the transition state to products drops below the reactant energy. Thus we can expect reactions to display a full range of behaviors between the two limiting cases presented so far. For example, the seemingly straightforward OH + HCl reaction clearly shows the influence of a van der Waals complex in its low-temperature behavior.[40,41] Conversely, we cannot look to "unusual" reaction kinetics as evidence for a fundamentally different mechanism in a reaction (for example, addition vs abstraction).

The OH + acetone reaction plays a critical role in the troposphere, where it is involved in the release of free radicals in the remote troposphere.[42,43] An extensive and careful experiment by Crowley et al.[44] showed strikingly non-Arrhenius behavior in the rate constant, measured between 200 and 400 K. All temperature-dependent data for both acetone + OH and acetone-d_6 + OH are shown in Figure 7.[36,44−46] Though these data were originally interpreted as indicating a role for an OH addition channel at low temperatures, there is now a growing consensus that there are in fact two H-atom abstraction pathways combining to produce the observed behavior.[46−48] A hydrogen-bonded pathway has a negative activation energy but a low *A*-factor, just as with nitric acid, but direct abstraction from the methyl groups dominates at high temperature, despite a substantial barrier, because the vibrational confinement of the hydrogen-bonded transition state is relaxed in the direct abstraction from the methyl groups. Consequently, the view that the extreme curvature reveals two separate rate constants is correct, but both specific reactions lead to identical products.

3.2. Radical Addition

Of course, radical addition to unsaturated molecules is an important mechanism. A large portion of the reactions responsible for both ozone formation and organic aerosol formation in the lower troposphere involve the oxidation of alkenes. Nearly one-third of the carbon flux into the atmosphere is in the form of isoprene, which reacts with OH on essentially every collision.[49−51] For a linear radical capable of rotation in two degrees of freedom, reaction near the collision frequency is no mean feat—it requires a transition state with substantially unhindered rotations, very loose or very extended or both. However, there is a large body of evidence indicating that the basic physics controlling radical addition reactions is identical to the atom abstraction case we just explored, involving barrier-height control by excited-state energy changes (primarily ionic, as we shall see), coupled to the emergence of pre-reactive complexes in systems with strong dipole and π mixing interactions. This is a dilemma; on the one hand these additions should have a barrier, and on the other hand they are apparently barrierless.

To solve the puzzle, we rely on several connected threads: First, we require the model of a mixed excited state comprising an ionic and a covalent (triplet) component, as in eq 4. Second, we need to fully understand the role of delocalization both in the mixed state and in the overall coupling at the avoided

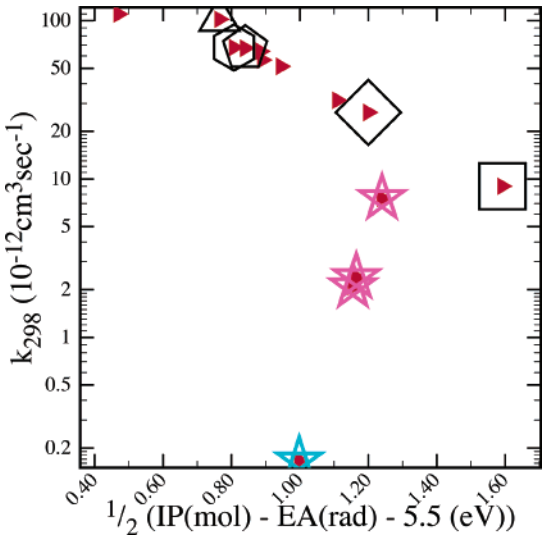

Figure 8. Room-temperature rate constants of OH + alkene reactions at the high-pressure limit[28] vs a crude measure of crossing height (0.5 × (IP−EA − 5.5 eV)). The main sequence is for unsubstituted alkenes and extends from ethene (square open symbol), through propene (diamond), cyclopentene and cyclohexene (pentagon and hexagon), to isoprene (triangle), displaying increasing reactivity with decreasing IP−EA, as expected. The stars are haloalkenes, which show greatly suppressed reactivity. OH + perchloroethylene (cyan star) is unique for the set in having a positive activation energy.

crossing. Third, as with H-atom abstraction, the key will be to explore how different *radicals* behave as much as to explore how different molecules behave.

We shall first consider a completely empirical plot of the room-temperature rate constant, k_{298}, for a series of OH radical−alkene reactions at their high-pressure limit vs IP−EA, shown in Figure 8. This is similar to Figure 7 in the article by Abbatt and Anderson.[20] The parameter has been scaled by subtracting 5.5 eV and dividing by 2 to make it a crude measure of crossing height, but in this form it remains purely empirical. The use of k_{298} instead of barrier height is justified by the coupled relationship between barrier heights and the lowest frequency modes at the transition state, which we have already discussed.[11] Because the pre-factor and barrier are controlled by common physics, we can, when necessary, look at rate constant trends in lieu of barrier trends.

There are two clear features in Figure 8. First, the unsubstituted alkenes organize tightly along a clear trend line, with room-temperature reactivity increasing by more than an order of magnitude from ethene at 1.6 eV to isoprene at 0.8 eV. Second, the haloalkenes shown here stand out as anomalously unreactive; the haloalkenes in general exhibit low reactivity.[21] They are indicated with stars in Figure 8. The OH + perchloroethylene reaction is shown with a cyan star; it is more than 100 times less reactive than the empirical trend would predict. The reaction is also nearly unique in the family of OH + alkene reactions in showing a positive temperature dependence.[28,52] This anomalous behavior turns out to be a key to understanding the complete system. Conversely, understanding this anomalous reactivity will

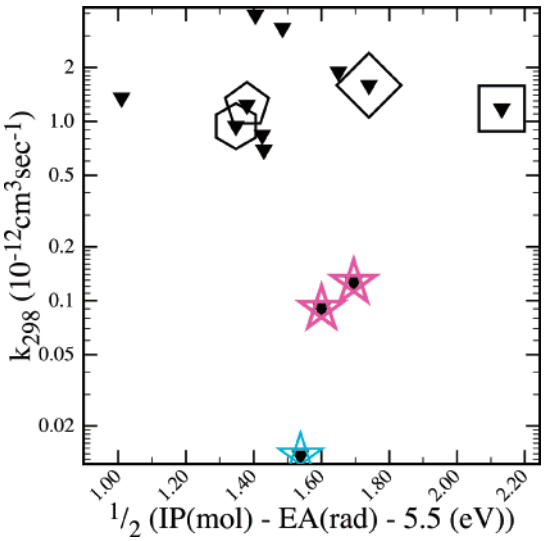

Figure 9. Room-temperature rate constant of H + alkene reactions[18] vs a crude measure of crossing height (0.5 × (IP−EA − 5.5 eV)), similar to Figure 8. The main sequence is less organized than for OH reactions, indicating involvement from other processes. The most striking feature, however, is again the suppression in haloalkene reactivity.

help us understand the behavior of persistent halogenated pollutants.

Rather than directly considering the OH reactions, we shall address H-atom additions to alkenes, discussed in the work of Clarke et al.[18,19] An empirical plot akin to Figure 8 for the reactions considered by Clarke et al. is shown in Figure 9. The dominant feature is again a factor of 100 suppression in the rate for H + perchloroethylene. *All* of these reactions show a positive temperature dependence, so they are relatively easy to model with a simple curve-crossing treatment and transition state theory. The measure of success (and the source of understanding) is to explain the suppression in haloalkene reactivity.

These systems demand consideration of more than one excited state.[19] In particular, Figure 10 shows a basic schematic of the important diabatic states. The diabatic interaction of the radical singly occupied molecular orbital (SOMO) with the alkene π-bond (shown in blue) is antibonding, while the diabatic potential associated with *removing* the radical from the adduct species (shown in green) clearly involves the molecular triplet. However, a third diabatic state can be identified with the reactant ionic states (for completeness, Clarke[19] considered two ionic states of opposite polarity). For many systems, the diabatic well (shown in green) is of order 95 kcal/mol (400 kJ/mol) deep, while the adiabatic well (from the green adduct to the blue reactant ground state) is of order 35 kcal/mol (150 kJ/mol) deep. Any changes in this basic picture for reactions such as those shown in Figures 8 and 9, considering only the green and blue curves, is quite subtle. The ionic state (shown in red), however, varies dramatically among these systems. This is qualitative evidence that the extreme variation in rate constants (4 orders of magnitude) shown in Figures 8 and 9 must be driven by the ionic term. To treat the system quantitatively with a two-state curve-crossing model, Clarke[19] combined these excited states into a single mixed state using eq 4.

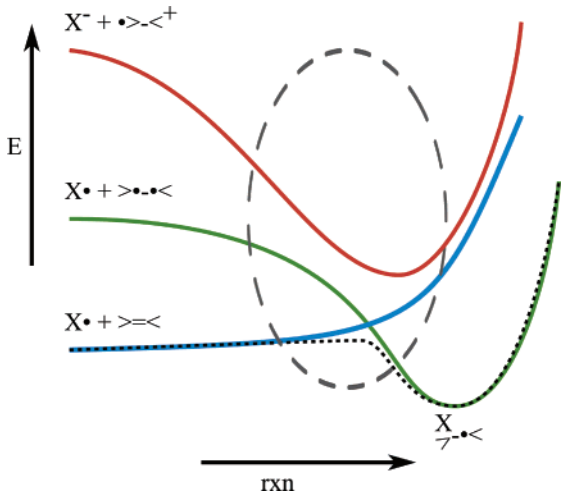

Figure 10. Basic potential energy surface for radical addition to alkenes. The diabatic interaction of the reactants (blue) is antibonding. The diabatic dissociation of the adduct (green) leads to a molecular triplet. These states stay at nearly fixed energy through many homologous series. The upper ionic state (red) varies considerably from reaction to reaction.

There are two consequences of the mixed excited state. The first is relatively obvious: for fixed overlap between the initial excited states and the ground state, increasing the energy of either excited state will increase the mixed-state energy, the crossing height, and the barrier. However, two things will happen if the frontier-orbital overlap changes between one of the excited states and the ground state. The mixed-state energy will change because overlap enters directly into eq 4, and the resonant splitting β at the curve-crossing will change as well. If the upper excited-state overlap drops, the individual effects are somewhat counterintuitive, though the overall effect is not. In particular, decreasing the overlap of the upper excited state with the ground state lowers the mixed excited-state energy but decreases the splitting by a larger factor (the mixed-state approximation is valid only for strong coupling, where β is substantially greater than 0.5). Consequently, the net effect of reducing this overlap is to increase the barrier height.

This is precisely what happens with the haloalkenes.[19,20] Figure 11 shows schematically the frontier-orbital occupancy (HOMO and LUMO) for ethene and perchloroethylene on only the olefinic carbons. The electronegative chlorines remove substantial electron density from the HOMO but leave the LUMO largely untouched. Because the singlet−triplet interaction involves components from both the HOMO and LUMO but the ionic interaction involves only the HOMO, the ionic-state overlap is much more sharply reduced by the substitution. This *lowers* the mixed-state energy (all else being equal). However, by far the largest effect of the reduced HOMO occupancy is to reduce the resonance splitting. Figure 12 shows the net result, with measured vs predicted barriers and a linear fit of the two—it follows the treatment described by Clarke,[19] differing in two ways. We have omitted a second (higher energy) ionic excited state (alkene$^-$ + H$^-$), found to have little influence, and we have explicitly incorporated strong coupling ((1

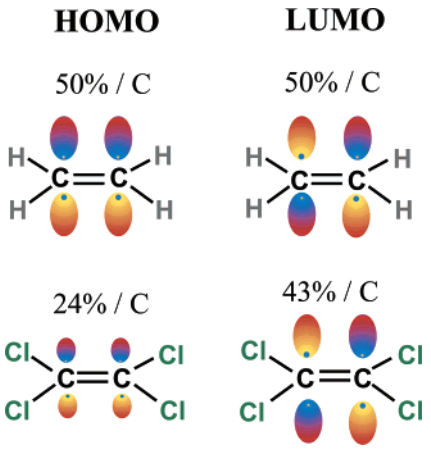

Figure 11. HOMO/LUMO occupancy on the olefinic carbons for ethene and perchloroethylene. Perchloroethylene is significantly less reactive than ethene. Reduced HOMO occupancy on perchloroethylene reduces the splitting at the avoided curve-crossing, thus increasing the barrier height for all radical reactions with perchloroethylene.

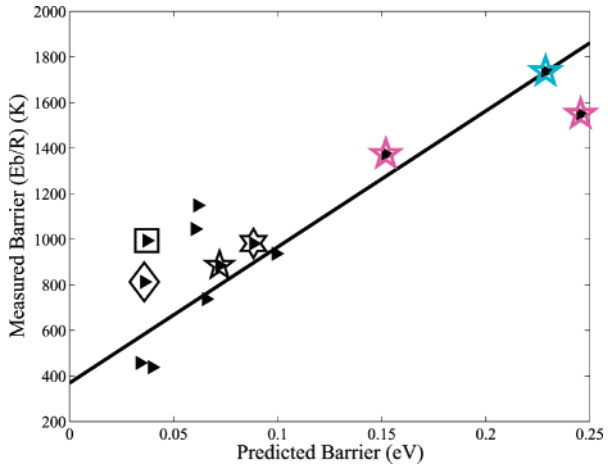

Figure 12. Evolution of barrier heights in a mixed excited-state curve-crossing model of H + alkene reactions, including haloalkenes (indicated with five-pointed colored stars). The reactions are the same reactions shown in Figure 9. The low haloalkene reactivity results from high (~1500 K) barriers, which are reproduced in the curve-crossing theory.

$- \beta) \propto 1/S^2$) into the model. The difference between Figures 9 and 12 is striking—in particular, the low reactivity of the haloalkenes has been quantitatively explained. In this case it is not variation in the excited-state energy but rather variation in splitting that drives the barrier-height change. The effect of halogen substitution is thus to reduce the ability of the ionic state to stabilize the transition state by reducing the overlap with the reactant ground state, consistent with frontier-orbital theory.[53]

The most difficult theoretical issue in this discussion concerns OH + alkene reactions. There is clear experimental and theoretical evidence that the smaller, less reactive alkenes include a barrier on the potential energy surface. The activation energy for OH + perchloroethylene is positive.[54] Even reactions with higher rate constants exhibiting a negative temperature dependence show "submerged" barriers in computational studies. For example, Abbatt[20] found a barrier following a deep pre-reactive complex on the OH + ethene potential energy surface. Recent studies of the potential energy surface for the OH + isoprene reaction show no signs of a barrier[51]—to locate an entropic transition state for master equation calculations, they fit a simple Morse potential to the adiabatic surface.

Alkene reactions with H atoms and OH radicals share common controlling physics, just like alkane reactions. There is also considerable evidence that pre-reactive complexes play a vital role in OH kinetics.[12] There is a clear empirical link between OH−alkene reactivity and H−alkene reactivity, and the basic frontier-orbital control originally articulated by Abbatt[20] for OH reactions has been affirmed by Clarke[19] for H-atom reactions. What remains unclear to date is how the controlling physics is manifest in OH−alkene reactions—whether a "submerged" barrier is present in unsubstituted alkenes, or whether the excited states have come sufficiently close to the ground-state surface to completely eliminate the barrier. The OH−alkene addition rate constants continue to get faster with decreasing ionization potential, as shown in Figure 8, even though the *activation energies* for most of these reactions are generally constant and consistent with a barrierless addition.[28] We have shown that the physics controlling barrier heights also controls the key bending frequency at the transition state—the *width* of the reactive channel. It is thus reasonable to hypothesize that, even after the rate-limiting transition state has settled at a point associated with barrierless adduct formation, the width (hindrance parameter) of this transition state is still controlled by the curve-crossing physics described here. This hypothesis, however, remains unproven.

The overall relationship between abstraction reactions and addition reactions is summarized in Figure 13. This figure shows the approximate energies of the unmixed ionic and triplet excited states involved in the reactions for unsubstituted alkanes and alkenes. The "triplet" state energy is equal to three-fourths of the singlet−triplet gap of the molecule, based on conservation of an overall spin of $^1/_2$ for the system,[55] while the "ionic" state energy accounts for Coulombic stabilization in the far field.[6] Each set of reactions forms a well-organized group with a nearly constant triplet energy: the alkanes at approximately 6 eV and the alkenes at approximately 3 eV. This figure shows how variation in the ionic energy of these systems is dramatically more significant than variation in the triplet energy. Ionic energy variation dominates barrier-height changes in two ways: first, the ionic energy is simply an order of magnitude more variable than the triplet energy; second, the bulk of the systems lie to the upper left of the 1:1 dividing line shown in gray, meaning that the ionic state at the curve-crossing boundary generally lies below the triplet state. Consequently, variability in reactivity *within* a given homologous series is dominated by variability in the ionic-state energies.

If one asks, however, why addition reactions to alkenes are generally faster than abstractions from alkanes, the answer is different. As Figure 13 clearly

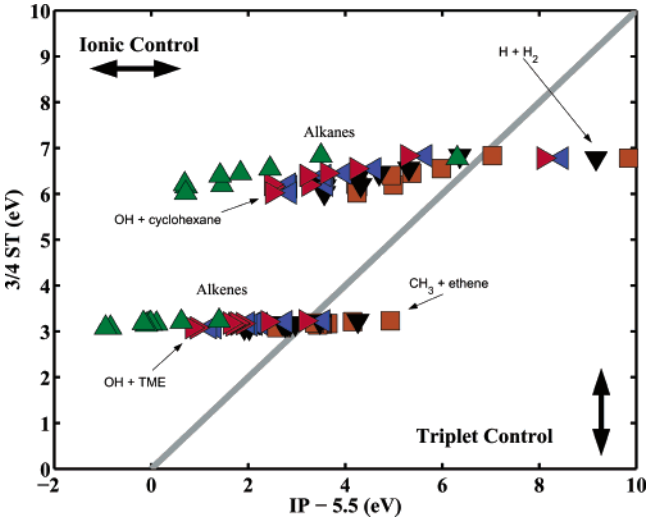

Figure 13. Approximate initial ionic and covalent (triplet) energies at the onset of the transition-state region (curve-crossing boundary) for a series of H-atom abstractions from alkanes (upper data) and radical additions to alkenes (lower data). Included in the "alkanes" is H_2, which appears to the far right. Different radicals are shown with different colors and symbol shapes; the set shown here is methyl (brown square), H (black downward-facing triangle), $O(^3P)$ (blue left-facing triangle), OH (red right-facing triangle), and Cl (green upward-facing triangle). Horizontal displacement reveals ionic control, while vertical displacement reveals triplet control. In addition, the diagonal 1:1 line (gray) divides a region to the upper left, where the ionic surface lies below the triplet surface at the curve-crossing boundary, from a region to the lower right, where the reverse is true.

shows, *both* ionic and triplet energies drop on going from abstraction to addition. Most of the reactions remain in the general region of ionic control, and so perhaps the ionic energy decline is more significant than the triplet energy decline, but both clearly contribute to the drop in barrier heights. Some of the systems (for instance, Cl + large alkenes) fall in a regime where the ionic energy is nominally *negative*, a potential onset of electron-jump, or harpoon behavior.[56] The ionic term clearly dominates here, and this suggests why the barriers for some OH-addition reactions may indeed have almost completely vanished from some reaction coordinates.

Figure 13 motivates a final point. A great deal of early theoretical consideration for both H-atom abstractions and radical additions was devoted to systems appearing on the right-hand limit of these collections—in particular H + H_2,[1,57] and R + alkenes.[16] The general conclusion was that singlet−triplet interactions dominate barrier-height formation. The ionic interactions ruling this discussion generally appeared as a perturbation. That conclusion was correct for those particular reactions. However, those reactions are not representative of either sequence, and the variation among reactions in each sequence is driven almost entirely by variation in the ionic-state energies.

4. Conclusions

In the broadest terms, radical−molecule barrier heights and reactivity are controlled by four factors:

- variation in the excited-state energies driving variation in the crossing height of two states related to the reactant and product configurations,
- tight correlation among transition-state energies, bending frequencies, and imaginary frequencies, causing a tight correlation between *A*-factors and activation energies,
- variation in the reactant ground-state interactions defining the initial lower boundary condition of the curve-crossing, most notably when those interactions are sufficiently strong to enable a stable pre-reactive complex and a correspondingly lower curve-crossing, and
- variation in frontier-orbital overlap driving variation in the coupling parameter, or stabilization at the avoided curve-crossing, most notably when depleted overlap reduces the coupling and thus increases the barrier height.

Chemical intuition based on properties of separated reactants and products can be used to define energies and coupling constants bounding a curve-crossing problem spanning the transition state. Careful treatment of the coupled problem demands clear delineation of the diabatic states and their subsequent mixing.[9] However, these coupled effects can be related transparently to causes rooted in the separated species.

Also in broad terms, these factors are listed roughly in order. Excited-state variation dominates variation *within* a given homologous series and also *among* different reaction classes. Significant stabilization of the ground state—for example, through hydrogen bonding between OH and a neighboring oxygen on the reactant molecule in the case of nitric acid, acetone, and other carbonyls—can cause dramatic effects, such as strongly negative activation energies. These effects generally seem anomalous, as they herald a departure from the regular sequence established by the excited-state variations. Physically, however, they represent a smooth transition and not a sharp departure. Finally, overlap-driven coupling changes *can* cause enormous changes in reactivity. In this article we are considering strongly coupled systems with coupling constants in the range 0.8−0.9. Decreasing this coupling obviously has the potential to increase barrier heights by a factor of 10, and to decrease reactivity by vastly more as reactions become Woodward−Hoffmann forbidden[3] and Born−Oppenheimer breakdown prevents transitions to the ground-state product surface.[58] The reactions we are considering are by their nature more strongly coupled than this, but we have seen in the haloalkenes that these effects can still change reactivity by more than a factor of 100.

By virtue of the strong variation in ionization potentials among similar molecules, as well as significant variation in the electron affinity of various radicals, variations in *ionic* excited-state energies dominate barrier-height changes in these neutral systems. The systems discussed here illustrate the fundamental phenomena because they exhibit a wide range of behavior and are relatively easy to study; the physics must extend to far more experimentally challenging systems, such as O_2 + RO reactions[30] and

internal atom shifts including the 1−5 H-atom shift in alkoxy radicals[54,59] and the internal H-atom transfer in the carbonyl oxides intermediates thought to dominate the ozonolysis of alkenes.[60−63]

Another area of emerging interest is the reactivity of radicals on aerosol surfaces. Of particular interest is the reactivity of organic species on these surfaces. Rudich and co-workers[64−66] and Molina and co-workers[67] have found that radical reactivity on surface-adsorbed organics is enhanced (when measured as a reaction probability per collision) relative to gas-phase reactivity (when measured as a fraction of the collision rate), with an enhancement that is roughly inversely proportional to gas-phase radical reactivity (i.e., nitrate radical and ozone have high enhancements, whereas OH and Cl have low enhancements). The physics governing the reaction potential energy surface should once again be similar to that described here, though the boundary conditions will be modified by interactions with the substrate and surrounding species. A theoretical explanation of this reactivity increase is a first-order need.

5. Acknowledgment

The work described here from the author's own research has been supported by a succession of grants from the National Science Foundation to Harvard and Carnegie Mellon Universities. The most recent is ATM-0125283. Numerous people have contributed significantly to that work, including (but not limited to) Jim Anderson, Jon Abbatt, Manvendra Dubey, Jim Clarke, and Heather Rypkema.

6. References

(1) Heitler, W.; London, F. *Z. Phys. Chem.* **1927**, *44*, 455.
(2) Fukui, K.; Fujimoto, H. *Bull. Chem. Soc. Jpn.* **1969**, *42*, 3399.
(3) Woodward, R. B.; Hoffman, R. *The Conservation of Orbital Symmetry;* Verlag Chemie: Weinheim, Germany, 1970.
(4) Pross, A. *Adv. Phys. Org. Chem.* **1985**, *21*, 99.
(5) Shaik, S. S.; Hiberty, P. C. *Adv. Quantum Chem.* **1995**, *26*, 99.
(6) Donahue, N. M.; Demerjian, K. L.; Anderson, J. G. *J. Phys. Chem. A* **1998**, *102*, 3121.
(7) Evans, M. G.; Polanyi, M. *Trans. Faraday Soc.* **1938**, *34*, 11.
(8) Marcus, R. A. *J. Chem. Phys.* **1956**, *24*, 966.
(9) Rypkema, H. A.; Donahue, N. M.; Anderson, J. G. *J. Phys. Chem. A* **2001**, *105*, 1498.
(10) Hammond, G. S. *J. Am. Chem. Soc.* **1955**, *77*, 334.
(11) Donahue, N. M. *J. Phys. Chem. A* **2001**, *105*, 1489.
(12) Smith, I. W. M.; Ravishankara, A. R. *J. Phys. Chem. A* **2002**, *106*, 4798.
(13) Marcus, R. A. *J. Phys. Chem.* **1968**, *72*, 891.
(14) Hammett, L. P. *J. Am. Chem. Soc.* **1937**, *59*, 96.
(15) Russell, G. A. *J. Am. Chem. Soc.* **1956**, *78*, 1047.
(16) Wong, M. W.; Pross, A.; Radom, L. *J. Am. Chem. Soc.* **1993**, *115*, 11050.
(17) Clarke, J.; Kroll, J.; Donahue, N.; Anderson, J. *J. Phys. Chem. A* **1998**, *102*, 9847.
(18) Clarke, J. S.; Kroll, J. H.; Rypkema, H. A.; Donahue, N. M.; Anderson, J. G. *J. Phys. Chem. A* **2000**, *104*, 9847.
(19) Clarke, J. S.; Rypkema, H. A.; Kroll, J. H.; Donahue, N. M.; Anderson, J. G. *J. Phys. Chem. A* **2000**, *104*, 5254.
(20) Abbatt, J. P. D.; Anderson, J. G. *J. Phys. Chem.* **1991**, *95*, 2382.
(21) Dubey, M. K.; Hanisco, T. F.; Wennberg, P. O.; Anderson, J. G. *Geophys. Res. Lett.* **1996**, *23*, 3215.
(22) Skodje, R. T.; Truhlar, D. G. *J. Phys. Chem.* **1981**, *85*, 624.
(23) Michelsen, H. A.; Simpson, W. R. *J. Phys. Chem. A* **2001**, *105*, 1476.
(24) Donahue, N. M.; Clarke, J. S. *Int. J. Chem. Kinet.* **2003**, in press.
(25) Nicovich, J. M.; van Dijk, C. A.; Kreutter, K. D.; Wine, P. H. *J. Phys. Chem.* **1991**, *95*, 9890.
(26) Seakins, P. W.; Pilling, M. J.; Niiranen, J. T.; Gutman, D.; Kransnoperov, L. N. *J. Phys. Chem.* **1992**, *96*, 9847.
(27) Dobis, O.; Benson, S. W. *J. Phys. Chem. A* **1997**, *101*, 6030.
(28) Atkinson, R.; Baulch, D. L.; Cox, R. A.; Crowley, J. N.; Hampson, R. F., Jr.; Kerr, J. A.; Rossi, M. J.; Troe, J. *Summary of Evaluated Kinetic and Photochemical Data for Atmospheric Chemistry*; Technical Report, IUPAC Subcommittee on Gas Kinetic Data Evaluation for Atmospheric Chemistry, 2002 (http://www.iupac-kinetic.ch.cam.ac.uk/).
(29) Wang, C.; Shemesh, L. G.; Deng, W.; Lilien, M. D.; Dibble, T. S. *J. Phys. Chem. A* **1999**, *103*, 8207.
(30) Deng, W.; Davis, A. J.; Zhang, L.; Katz, D. R.; Dibble, T. S. *J. Phys. Chem. A* **2001**, *105*, 8985.
(31) Sander, S. P.; Friedl, R. R.; DeMore, W. B.; Golden, D. M.; Kurylo, M. J.; Hampson, R. F.; Huie, R. E.; Moortgat, G. K.; Ravishankara, A. R.; Kold, C. E.; Molina, M. J. *Chemical Kinetics and Photochemical Data for Use in Stratospheric Modeling Supplement to Evaluation 12: Update of Key Reactions*, Evaluation No. 13; JPL Technical Report 00-3; Jet Propulsion Laboratory: Pasadena, CA, 2000 (and references therein).
(32) Brown, S. S.; Talukdar, R. K.; Ravishankara, A. R. *J. Phys. Chem. A* **1999**, *103*, 3031.
(33) Mozurkewich, M.; Benson, S. W. *J. Phys. Chem.* **1984**, *88*, 6429.
(34) Lamb, J. J.; Mozurkewich, M.; Benson, S. W. *J. Phys. Chem.* **1984**, *88*, 6441.
(35) Tsiouris, M.; Wheeler, M. D.; Lester, M. I. *J. Chem. Phys.* **2001**, *114*, 187.
(36) Calvé, S. L.; Hitier, D.; Bras, G. L.; Mellouki, A. *J. Phys. Chem. A* **1998**, *102*, 4579.
(37) Holbrook, K., Pilling, M., Robertson, S., Eds.; *Unimolecular Reactions*; John Wiley & Sons: London, 1996.
(38) Barker, J. R. *Int. J. Chem. Kinet.* **2002**, *33*, 232.
(39) Barker, J. R.; Golden, D. M. *Chem. Rev.* **2003**, *103*, 4577 (in this issue).
(40) Sharkey, P.; Smith, I. W. M. *J. Chem. Soc., Faraday Trans.* **2002**, *89*, 1993.
(41) Battin-Leclerc, F.; Kim, I. K.; Talukdar, R. K.; Portmann, R. W.; Ravishankara, A. R.; Steckler, R.; Brown, D. *J. Phys. Chem. A* **1999**, *103*, 3237.
(42) Wennberg, P. O.; et al. *Science* **1998**, *279*, 49.
(43) Jaegle, L.; et al. *Geophys. Res. Lett.* **1997**, *24*, 3181.
(44) Wollenhaupt, M.; Carl, S. A.; Horowitz, A.; Crowley, J. N. *J. Phys. Chem. A* **2000**, *104*, 2695.
(45) Wallington, T. J.; Kurylo, M. J. *J. Phys. Chem.* **1987**, *91*, 5050.
(46) Yamada, T.; Taylor, P. H.; Goumri, A.; Marshall, P., 2003, in press.
(47) Masgrau, L.; Gonzalez-Lafont, A.; Lluch, J. M. *J. Phys. Chem. A* **2002**, *106*, 11760.
(48) Talukdar, R. K.; Gierczak, T.; McCabe, D. C.; Ravishankara, A. R. *J. Phys. Chem. A* **2003**, *107*, 5021.
(49) Chuong, B.; Stevens, P. S. *J. Phys. Chem. A* **2000**, *104*, 5230.
(50) Campuzano-Jost, P.; Williams, M. B.; D'Ottone, L.; Hynes, A. J. *Geophys. Res. Lett.* **2000**, *27*, 693.
(51) McGivern, W. S.; Suh, I.; Clinkenbeard, A. D.; Zhang, R.; North, S. W. *J. Phys. Chem. A* **2000**, *104*, 6609.
(52) Tichenor, L. B.; Graham, J. L.; Yamada, T.; Taylor, P. H.; Peng, J.; Hu, X.; Marshall, P. *J. Phys. Chem. A* **2000**, *104*, 1700.
(53) Fujimoto, H.; Yamabe, S.; Fukui, K. *Bull. Chem. Soc. Jpn.* **1971**, *44*, 2936.
(54) Atkinson, R. *J. Phys. Chem. Ref. Data* **1994**, *Monograph 2*, 216 pp.
(55) Shaik, S. S.; Hiberty, P. C.; Lefour, J.-M.; Ohanessian, G. *J. Am. Chem. Soc.* **1987**, *109*, 363.
(56) Herschbach, D. R. *Adv. Chem. Phys.* **1966**, *10*, 319.
(57) Porter, R. N.; Karplus, M. *J. Chem. Phys.* **1964**, *40*, 1105.
(58) Mueller, J. A.; Morton, M. L.; Curry, S. L.; Abbatt, J. P. D.; Butler, L. J. *J. Phys. Chem. A* **2000**, *104*, 4825.
(59) Ferenac, M. A.; Davis, A. J.; Holloway, A. S.; Dibble, T. S. *J. Phys. Chem. A* **2003**, *107*, 63.
(60) Gutbrod, R.; Schindler, R. N.; Kraka, E.; Cremer, D. *Chem. Phys. Lett.* **1996**, *252*, 221.
(61) Olzmann, M.; Kraka, E.; Cremer, D.; Gutbrod, R.; Andersson, S. *J. Phys. Chem. A* **1997**, *101*, 9421.
(62) Paulson, S. E.; Chung, M. Y.; Hassan, A. S. *J. Phys. Chem. A* **1999**, *103*, 8125.
(63) Kroll, J. H.; Cee, V. J.; Donahue, N. M.; Demerjian, K. L.; Anderson, J. G. *J. Am. Chem. Soc.* **2002**, *124*, 8518.
(64) Thomas, E. R.; Frost, G. J.; Rudich, Y. *J. Geophys. Res.* **2001**, *106*, 3045.
(65) Moise, T.; Talukdar, R. K.; Frost, G. J.; Fox, R. W.; Rudich, Y. *J. Geophys. Res.* **2002**, *107*, AAC 6-1.
(66) Moise, T.; Rudich, Y. *J. Phys. Chem. A* **2002**, *106*, 6469.
(67) Bertram, A. K.; Ivanov, A. V.; Hunter, M.; Molina, L. T.; Molina, M. J. *J. Phys. Chem. A* **2001**, *105*, 9415.

CR020650G